Molecular Cloning of Integrin-associated Protein: An Immunoglobulin Family Member with Multiple Membrane-spanning Domains Implicated in $\alpha_v\beta_3$-dependent Ligand Binding

Frederik P. Lindberg, Hattie D. Gresham,* Elsa Schwarz, and Eric J. Brown

The Division of Infectious Diseases, Department of Medicine, and the Departments of Cell Biology and Physiology and Molecular Microbiology, Washington University School of Medicine, St. Louis, Missouri 63110; and *Harry S. Truman Veterans' Administration Hospital, and Departments of Pharmacology and Molecular Microbiology and Immunology, University of Missouri, Columbia, Missouri 65201

Abstract. Integrin Associated Protein (IAP) is a 50-kD membrane protein which copurifies with the integrin $\alpha_v\beta_3$ from placenta and coimmunoprecipitates with β_3 from platelets. IAP also is functionally associated with signal transduction from the Leukocyte Response Integrin. Using tryptic peptide sequence, human and murine IAP cDNAs have been isolated. The protein has an extracellular amino-terminal immunoglobulin domain that binds all monoclonal anti-IAP antibodies. The carboxy-terminal region is highly hydrophobic with three or five membrane-spanning segments and a short hydrophilic tail. Immunofluorescence microscopy suggests that this hydrophilic tail is located on the inside of the cytoplasmic membrane. Monoclonal anti-IAP antibody inhibits the binding of vitronectin-coated beads to $\alpha_v\beta_3$ on human erythroleukemia cells, and polyclonal anti-IAP recognizes hamster IAP on CHO cells and inhibits vitronectin bead binding. When CHO cells are transfected with human IAP, monoclonal anti-human antibody completely inhibits vitronectin bead binding. These data suggest a model in which ligand binding by $\alpha_v\beta_3$ is regulated by IAP.

ADHESION receptors of the integrin family recognize several proteins of the extracellular matrix and appear to be critical for the induction of normal morphology and migration of many cell types (2, 4, 6, 22, 31). While the interaction of integrins with their ligands has been the subject of intense study over the past several years, much less information has been gathered about the molecular mechanisms by which integrins affect cell phenotype and function. Recently, we described a cell surface protein which we copurified with the integrin $\alpha_v\beta_3$ from placenta and which also coimmunoprecipitated with β_3 integrins from platelets (5). This coprecipitating protein had a M_r of ~50 kD on SDS-PAGE, was highly hydrophobic, and was widely expressed. The 50-kD protein itself did not recognize the Arg-Gly-Asp peptides with which $\alpha_v\beta_3$ was purified (5), but mAb recognizing the 50-kD protein could inhibit several neutrophil and monocyte functions mediated by a leukocyte β_3-like integrin, including ligand binding (5, 16, 17, 35). Therefore, we hypothesized that the 50-kD protein, which we called Integrin-associated Protein (IAP),[1] could physically associate with some integrins and, without directly binding the integrin ligands, could regulate integrin function. Now, we have cloned IAP cDNA from both human and mouse cells and examined its structure and role in binding vitronectin (Vn) ligand in native and transfected cells.

Materials and Methods

Tissue Culture

Tissue culture cells were grown at 37°C, 5% CO_2, in Iscove's Modified Dulbecco's Medium (GIBCO BRL, Gaithersburg, MD), supplemented with 10% FCS (Hyclone Labs., Logan, UT). For bead binding, CHO cells were grown in Ham's F12 with 10% FCS supplemented with 250 μg/ml active G418.

Antibodies

The mouse IgG*1* anti-IAP mAbs used have been described previously (5, 16). B6H12, 1F7, 2B7, 2E11, and 3E9 are inhibitory to Leucocyte Response

Please address all correspondence to Dr. Eric Brown, Campus Box 8051, Washington University School of Medicine, 660 S. Euclid Avenue, St. Louis, MO 63110.

1. *Abbreviations used in this paper:* AI, attachment index; Fn, fibronectin; HEL, human erythroleukemia; HSA, human serum albumin; IAP, Integrin-associated Protein; LRI, Leucocyte Response Integrin; PMN, polymorphonuclear cell; Vn, vitronectin.

Integrin (LRI)-stimulation of Fc-receptor-mediated phagocytosis in neutrophils. 2D3 and 3G3 are non-inhibitory. All antibodies immunoprecipitate IAP. mAb 6F2 is an isotype matched control.

Preparation of Anti-Peptide Antibodies

A peptide, CNQKTIQPPRNN, was synthesized by the Washington University Protein Chemistry facility. This peptide corresponds to the carboxy-terminal 11 amino acids predicted by pIAP3, with an amino-terminal cysteine added for conjugation to keyhole limpet hemocyanin. Cross-linking was performed using the bifunctional cross-linker bromacetylsuccinimide, as previously described (16). Rabbits were immunized with 50 μg of the protein-peptide conjugate in complete Freund's adjuvant, and then 20 d later in incomplete Freund's adjuvant. Immunization in incomplete Freund's was continued on a monthly basis for 2 mo.

mAbs against the human IAP carboxy terminus were prepared as described (16) using 50 μg of the peptide conjugate per injection. The two mAbs used in this study both immunoprecipitate human IAP and bind to the human carboxy-terminal peptide. Miap151 also reacts with the corresponding peptide derived from the mouse sequence, whereas miap131 does not, demonstrating that the two mAbs have different antigen combining sites.

IAP Cloning

Standard techniques were used for cloning and other nucleic acid manipulation (32). A tryptic peptide sequence, VEFTFCNDTVVIPCFVTNMEAQ, was obtained from IAP purified from placenta, as previously described (5). Based on this sequence, two degenerate oligonucleotides were synthesized and used for PCR using a U937 CDNA library in λgt10 (the kind gift of Dr. Douglas Lublin, Washington University) as template. The forward oligonucleotide was 5′-GTIGA(ag)TT(tc)ACITT(tc)TG(tc)AA(tc)GA-3′, and the inverse was 5′-TGIGC(TC)TCCAT(ag)TTIGTIAC(ag)AA(ag)CA-3′. The PCR product of 66 bp was cloned into pBluescriptII-KS(+) (Stratagene, La Jolla, CA), sequenced (33) to confirm that it encoded the expected peptide, and used to probe the U937 cDNA library using conventional techniques. The *Eco*RI insert was subcloned from the phage into pBluescriptII-KS(+) resulting in pIAP0. A 5′-fragment (*Eco*RI-*Xmn*I) of the pIAP0 insert was used to screen a λZAPII (Stratagene) cDNA library from differentiated HL60 cells (the kind gift of Dr. Brian Volpp, University of Iowa), from which several clones containing the entire coding sequence were obtained. Two clones, pIAP3 and pIAP4, were sequenced to obtain unambiguous overlapping readings from both strands. Plasmid pIAP4 contains IAP with the longest 5′ untranslated sequence, but the plasmid also contains a second unrelated cDNA. Therefore, pIAP3 was used for all further studies. Several other clones were sequenced on one strand or partially. These clones varied in the length of their 5′ and 3′ untranslated sequences, but were identical to pIAP3 in the coding region to the extent of the sequence obtained. The sequence submitted to Genbank (Fig. 1; Accession number Z25521) is the synthesis of the sequences obtained from pIAP3 and pIAP4. Plasmid pIAP0 has a 32 bp deletion (Fig. 1) compared to pIAP3/pIAP4 at the 3′ end of the coding sequence, presumably due to alternative splicing.

Murine IAP cDNA was obtained by screening a cDNA library from the 70Z/3 pre-B cell line using the full length human IAP cDNA under conditions of intermediate stringency. One of the initial clones, pIAP28, was used for further study. The library was rescreened with a 5′ murine IAP probe to obtain clones with as much 5′ untranslated sequence as possible. The 5′ end of the clone with the longest 5′ untranslated sequence, pIAP42, was sequenced. The 5′ untranslated region of pIAP28 was identical to the corresponding region of pIAP42. The sequence submitted to Genbank (accession number Z25524) is the synthesis of the sequence obtained from pIAP28 and pIAP42.

Sequence Analysis

The National Center of Biotechnology Information (NCBI) electronic mail servers BLAST (25) and RETRIEVE were used to find and retrieve homologous sequences. Sequence comparison was done by the Needleman and Wunsch algorithm (10) with the protein alignment matrix PAM250, a bias of 10, and a gap penalty of 10. The result for a pair of sequences was given as standard deviations of the score above the mean of the alignment score for 150 random permutations of the same sequences. Hydrophobicity plots were calculated as described by Kyte and Doolittle (39) using a window of 11 residues.

Construction of IAP Expression Plasmids and Chimeric IAP Genes

pIAP3 was digested with *Hind*III and *Xba*I, which cut in the pBluescriptII-SK(−) polylinker just 5′ and 3′ of the insert, respectively. The resulting *Hind*III-*Xba*I fragment was ligated into pRC/RSV (Invitrogen, La Jolla, CA) digested with the same enzymes, yielding pIAP45. IAP was divided into three regions, delimited by stretches of amino acid sequence identity between the human and mouse variants. The delimiting sequences were chosen so that unique restriction sites could be introduced into the cDNAs, without altering the amino acid sequence. Using PCR, the gene segments were obtained individually, subcloned, and sequenced. Fig. 1 shows the doubly underlined regions of homology between the oligonucleotides used and the human IAP cDNA sequence. The letters labeling the regions are placed under the amino acids delimiting the segments. The corresponding point in the mouse sequence can be deduced from the alignment in Fig. 2. The 5′ hydrophobic segment encoding region (amino acids M^1–S^{18}) was obtained as an *Xba*I–*Bam*HI fragment (oligonucleotides 5′-GAAG TCTAGA CC ATG TGG CCC CTG GTA GCG-3′ and 5′-TAG CTG AGC GGATCC GCA GCA GC-3′ for human IAP, and 5′-GAAG TCTAGA CC ATG TGG CCC TTG GCG GCG-3′ and 5′-TAG TTG AGC GGATCC GCA GCA GC-3′ for mouse IAP; Fig 1. segment *a–b*). The DNA encoding the hydrophilic domain (S^{18}–W^{136}) was obtained as a *Bam*HI–*Pvu*II fragment (5′-CTGC GGATCC GCT CAG CTA CTA-3′ and 5′-GAAA CTG CAGCTG ACA ACA CGA TAT TTT AG-3′ for human IAP, and 5′-CTGC GGATCC GCT CAA CTA CTG-3′ and 5′-GAAA CTGCAGCTG ACT AAT TTG CAA CCT CC-3′ for murine IAP; Fig 1. segment *b–c*). The remaining part of the cDNA (W^{131}–N^{305}) was made as a *Pvu*II–*Hind*III fragment (5′-GTTG CTGCAGCTGG TTT TCT CCA AAT GAA-3′ and 5′CCC AAGCTT AGA TCT TTC ACG TCT TAC TAC TC-3′ for human IAP, and 5′-GTTG CTGCAGCTGG TTT TCT CCA AAT GAA-3′ and 5′-CCC AAGCTT AGAT CTC TGT ATT CTT CCA TTT CTG-3′ for mouse IAP; Fig 1. segment *c–d*). The three different fragments were assembled and put under the control of the T7 promoter in pBC-KS(−) (Stratagene, La Jolla, CA). The clones were designated pIAP57 (all human), pIAP79 (all murine), pIAP67 (human with murine hydrophilic region *b–c*), and pIAP76 (murine with human hydrophilic region *b–c*).

For transfection, the inserts from the various chimeric clones were obtained as *Hind*III–*Xba*I fragments and cloned into the expression vector pIAP58 (unpublished; pRC/RSV with a replaced polylinker reversing the order of the *Hind*III and *Xba*I sites), yielding plasmids pIAP70, pIAP83, pIAP72, and pIAP80, respectively. An anti-sense control construct, pIAP69, was constructed by cloning the all human insert into pRC/RSV.

FACScan and FACSorting

Fluorescent flow microcytometry was performed using anti-human IAP mAbs precisely as described (5). Before incubation with anti-IAP mAbs, CHO cells were removed from tissue culture plates by incubation with trypsin-EDTA and washed twice with PBS. For FACSorting, cells were removed from the plates using Dulbecco's PBS with 2 mM EDTA, stained, resuspended to 5×10^6 cells/ml, and sorted in an Epics 753 FACSorter. Generally, the 5% most fluorescent cells were recovered.

Transfection of CHO Cells

CHO cells were grown to 50% confluence in 35-mm diam dishes and transfected with 3 μg plasmid DNA using the calcium phosphate method (15). Cells were grown for 24 h in nonselective medium. They were then removed with trypsin-EDTA and seeded into 25 cm^2 flasks containing medium with 600 μg/ml active G418 (GIBCO BRL). After 14 d, the pool of survivors was analyzed by FACScan. For subsequent experiments, enrichment for expressors was carried out by FACSorting the 5% highest staining cells using an anti-IAP mAb (1F7) as primary antibody. Anti-sense and vector control transfectants were sorted similarly.

Immunoprecipitation

For immunoprecipitation, U937 cells, CHO cells, or platelets were labeled with biotin hydrazide. Cells were washed with biotinylation buffer (0.15 M NaCl, 0.05 M acetate, pH 5.5), incubated with 10 mM $NaIO_4$ in the same buffer for 30 min on ice, and washed with biotinylation buffer. Biotin hydrazide (2 μg/ml) was added and incubation continued for 1.5 h at 4°C. The cell pellet was subsequently washed twice with PBS and lysed in PBS containing 1% Triton X-100, 1% deoxycholate, and 2 mM PMSF. After centrifugation for 15 min at 15,000 *g* to remove cell debris, the lysate was used

for immunoprecipitation. 1 μl of rabbit serum was incubated with 20 μl protein A–Sepharose (Pharmacia LKB Biotechnology, Piscataway, NJ) or 100 μl of monoclonal antibody tissue culture supernatant was incubated with 20 μl anti-mouse IgG-Sepharose (Cappel Organon-Technica, West Chester, PA). The antibody-charged Sepharose was washed and added to 200 μl of cell lysate, incubated for 2 h to overnight at 4°C, washed twice with lysis buffer, and twice with PBS containing 0.05% Tween-20. The Sepharose pellet was heated to 65°C for 10 min in Laemmli buffer for SDS-PAGE (9), the sample electrophoresed through a 10% SDS-PAGE gel and transferred to polyvinylidine difluoride paper (Milipore, Bedford, MA). Immunoprecipitated proteins were detected using streptavidin conjugated to horseradish peroxidase (Jansen Biochimica, Belgium) and chemiluminescence peroxidase substrate (ECL, Amersham Corp., Arlington Heights, IL).

In Vitro Translation

Wild-type and mutant IAP cDNAs were cloned into pBluescriptII-KS(+) under the control of the phage T7-promoter. The plasmids were linearized at the 3′-end of IAP and in vitro transcribed by T7-RNA polymerase in the presence of 500 μM $m^7G(5')ppp(5')G$ cap analogue (New England Biolabs, Beverly, MA). The RNA was in vitro translated using rabbit reticulocyte lysate in the presence of [^{35}S]methionine (Amersham Corp.), and canine pancreatic microsomal membranes for cotranslational processing (Promega Corp., Madison, WI), according to the manufacturer's instructions. In vitro translated products were immunoprecipitated with various anti-IAP mAb or an isotype matched irrelevant control, as described above. Supernatants of negative immunoprecipitations were analyzed by SDS-PAGE to confirm the presence of an appropriate size in vitro translation product.

Preparation of Vitronectin-coated Beads

Ligand-coated beads were prepared by incubating 4 × 10^8 1.3 μm aldehyde-modified fluorescent latex beads (Molecular Probes, Eugene, OR) with 10 μg purified Vn (Telios Pharmaceuticals, San Diego, CA), fibronectin (Fn, Telios), or human serum albumin (HSA) as a control in 200 μl of PBS. After 1 h at 37°C, 10 mg of HSA in 800 μl PBS was added to quench unreacted sites. After 1 h the beads were washed and resuspended in 1 ml of HBSS containing divalent cations (see below) and 1% HSA. Immediately before use, the preparations were sonicated for 1–2 s to disrupt aggregates.

Vitronectin-bead Binding

Vn-bead and Fn-bead binding to human erythroleukemia (HEL) cells was assessed by a modification of the previously described assay (17). The standard incubation mixture contained 1.5 × 10^5 cells, various concentrations of antibodies, and 45 μl of ligand-coated beads in a volume of 130 μl. The incubation buffer for Vn-beads was HBSS with 1% HSA, 2 mM $CaCl_2$, 1 mM $MgCl_2$, and 1 mM $MnCl_2$. The incubation buffer for Fn-beads was identical except for omission of the $CaCl_2$ and $MgCl_2$. These divalent cation conditions allowed maximal binding of Vn-beads to $\alpha_v\beta_3$ and Fn-beads to $\alpha_5\beta_1$ without interaction with other cell surface receptors. For antibody inhibition studies, cells were incubated with various monoclonal and polyclonal antibodies for 15 min at room temperature and for 15 min before the addition of the beads. The antibodies used were rabbit nonimmune IgG (18 μg); rabbit anti-VnR (16) 1:100; rabbit IgG anti-IAP (18 μg); rabbit anti-FnR (Telios) 1:100; murine IgG*1* anti-IAP mAb 2D3 (22 μg); murine IgG*1* anti-IAP mAb B6H12 (22 μg); murine IgG*1* anti-β_3 mAb 7G2 (25 μg); and murine anti-α_5 IgG*3* mAb PlD6 (Telios, 1:100). After 1 h at 37°C, the cells were washed three times in PBS and the number of beads bound assessed by microscopy. Binding was quantitated as an attachment index (AI), the number of beads bound per 100 cells.

Binding experiments with CHO transfectants were performed essentially identically, except that 2 × 10^4 CHO cells were adhered to glass 4-chamber LabTek slides (Nunc Inc., Naperville, IL) overnight and used as adherent cells. The total volume of the reaction mixture in the LabTek chamber was 500 μl, and antibody additions were increased to keep the concentration similar to that used for the HEL cells in suspension.

Results

Cloning of IAP

To determine the structure of IAP, we cloned its cDNA from a U937 λgt10 cDNA library (27). Several cDNAs were analyzed which all ended at a 5′ *Eco*RI site within the open reading frame. PCR analysis of the cDNA library failed to reveal full length clones, presumably due to incomplete *Eco*RI methylation of the cDNA. Therefore, we probed a neutrophil-like DMSO-differentiated HL60 library (40) with a 5′ fragment of the partial cDNA from U937. Several longer clones were sequenced. They all encode an open reading frame of 305 amino acids (Fig. 1). As confirmation of the identity of the clone, several tryptic peptides obtained from purified protein were found in the predicted amino acid sequence of IAP (dashes above the sequence in Fig. 2; *top*). The translation initiation site shown in Fig. 1 conforms only poorly to the Kozak consensus (24). It is likely that this is the initiation site based on the absence of a preceding initiation codon in any of the clones, the highly abnormal amino acid sequence that would be encoded by the CGG repeats in the 5′ end, and the expression from the cDNA of a protein

```
-138  GCGTGCGCGCGGCCGTGCAGCCTGGGCAGTGGGTCCTGCCTGTGACGCGCGGCGGCGGTC   -79
 -78  GGTCCTGCCTGTAACGGCGGCGGCGGCTGCTGCTCCAGACACCTGCGGCGGCGGCGGCGA   -19

                        M  W  P  L  V  A  A  L  L  L  G  S  A  C     14
 -18  CCCCGCGGCGGGCGCGGAGATGTGGCCCCTGGTAGCGGCGCTGTTGCTGGGCTCGGCGTG     41
                    =(a)================                ====

  15   C  G  S  A  Q  L  L  F  N  K  T  K  S  V  E  F  T  F  C  N     34
  42  CTGCGGATCAGCTCAGCTACTATTTAATAAAACAAAATCTGTAGAATTCACGTTTTGTAA    101
      ======(b)=============

  35   D  T  V  V  I  P  C  F  V  T  N  M  E  A  Q  N  T  T  E  V     54
 102  TGACACTGTCGTCATTCCATGCTTTGTTACTAATATGGAGGCACAAAACACTACTGAAGT    161

  55   Y  V  K  W  K  F  K  G  R  D  I  Y  T  F  D  G  A  L  N  K     74
 162  ATACGTAAAGTGGAAATTTAAAGGAAGAGATATTTACACCTTTGATGGAGCTCTAAACAA    221

  75   S  T  V  P  T  D  F  S  S  A  K  I  E  V  S  Q  L  L  K  G     94
 222  GTCCACTGTCCCCACTGACTTTAGTAGTGCAAAAATTGAAGTCTCACAATTACTAAAAGG    281

  95   D  A  S  L  K  M  D  K  S  D  A  V  S  H  T  G  N  Y  T  C    114
 282  AGATGCCTCTTTGAAGATGGATAAGAGTGATGCTGTCTCACACACAGGAAACTACACTTG    341

 115   E  V  T  E  L  T  R  E  G  E  T  I  I  E  L  K  Y  R  V  V    134
 342  TGAAGTAACAGAATTAACCAGAGAAGGTGAAACGATCATCGAGCTAAAATATCGTGTTGT    401
                                                ================

 135   S  W  F  S  P  N  E  N  I  L  I  V  I  F  P  I  F  A  I  L    154
 402  TTCATGGTTTTCTCCAAATGAAAATATTCTTATTGTTATTTTCCCAATTTTTGCTATACT    461
      ===(c)================

 155   L  F  W  G  Q  F  G  I  K  T  L  K  Y  R  S  G  G  M  D  E    174
 462  CCTGTTCTGGGGACAGTTTGGTATTAAAACACTTAAATATAGATCCGGTGGTATGGATGA    521

 175   K  T  I  A  L  L  V  A  G  L  V  I  T  V  I  V  I  V  G  A    194
 522  GAAAACAATTGCTTTACTTGTTGCTGGACTAGTGATCACTGTCATTGTCATTGTTGGAGC    581

 195   I  L  F  V  P  G  E  Y  S  L  K  N  A  T  G  L  G  L  I  V    214
 582  CATTCTTTTCGTCCCAGGTGAATATTCATTAAAGAATGCTACTGGCCTTGGTTTAATTGT    641

 215   T  S  T  G  I  L  I  L  L  H  Y  Y  V  F  S  T  A  I  G  L    234
 642  GACTTCTACAGGGATATTAATATTACTTCACTACTATGTGTTTAGTACAGCGATTGGATT    701

 235   T  S  F  V  I  A  I  L  V  I  Q  V  I  A  Y  I  L  A  V  V    254
 702  AACCTCCTTCGTCATTGCCATATTGGTTATTCAGGTGATAGCCTATATCCTCGCTGTGGT    761

 255   G  L  S  L  C  I  A  A  C  I  P  M  H  G  P  L  L  I  S  G    274
 762  TGGACTGAGTCTCTGTATTGCGGCGTGTATACCAATGCATGGCCCTCTTCTGATTTCAGG    821

 275   L  S  I  L  A  L  A  Q  L  L  G  L  V  Y  M  K  F  V  A  S    294
 822  TTTGAGTATCTTAGCTCTAGCACAATTACTTGGACTAGTTTATATGAAATTTGTGGCTTC    881
                                                              ----

 295   N  Q  K  T  I  Q  P  P  R  N  N                          305
 882  CAATCAGAAGACTATACAACCTCCTAGGAATAACTGAAGTGAAGTGATGGACTCCGATTT    941
      ------------------------

 942  GGAGAGTAGTAAGACGTGAAAGGAATACACTTGTGTTTAAGCACCATGGCCTTGATGATT   1001
           ==================(d)=

1002  CACTGTTGGGGAGAAGAAACAAGAAAAGTAACTGGTTGTCACCTATGAGACCCTTACGTG   1061
1062  ATTGTTAGTTAAGTTTTTATTCAAAGCAGCTGTAATTTAGTTAATAAAATAATTATGATC   1121
1122  TAAAAAAAAA
```

Figure 1. Sequence of human IAP cDNA. Nucleotides are numbered relative to the start of the initiation codon. The cDNA ends with a short poly-A tail, preceded by a poly-adenylation site. Above the sequence the deduced amino acid sequence (in one-letter IUPAC code) is shown, starting with the initiator methionine. Regions homologous to the oligonucleotides used for construction of IAP chimeras (see Materials and Methods) are doubly underlined. In each case, the letter naming the region indicates the point of fusion between the PCR fragments. The singly underlined sequence is the region absent from the U937 clone and a small minority of the HL60 clones. This would lead to a protein terminating in $K^{290}FVE$.

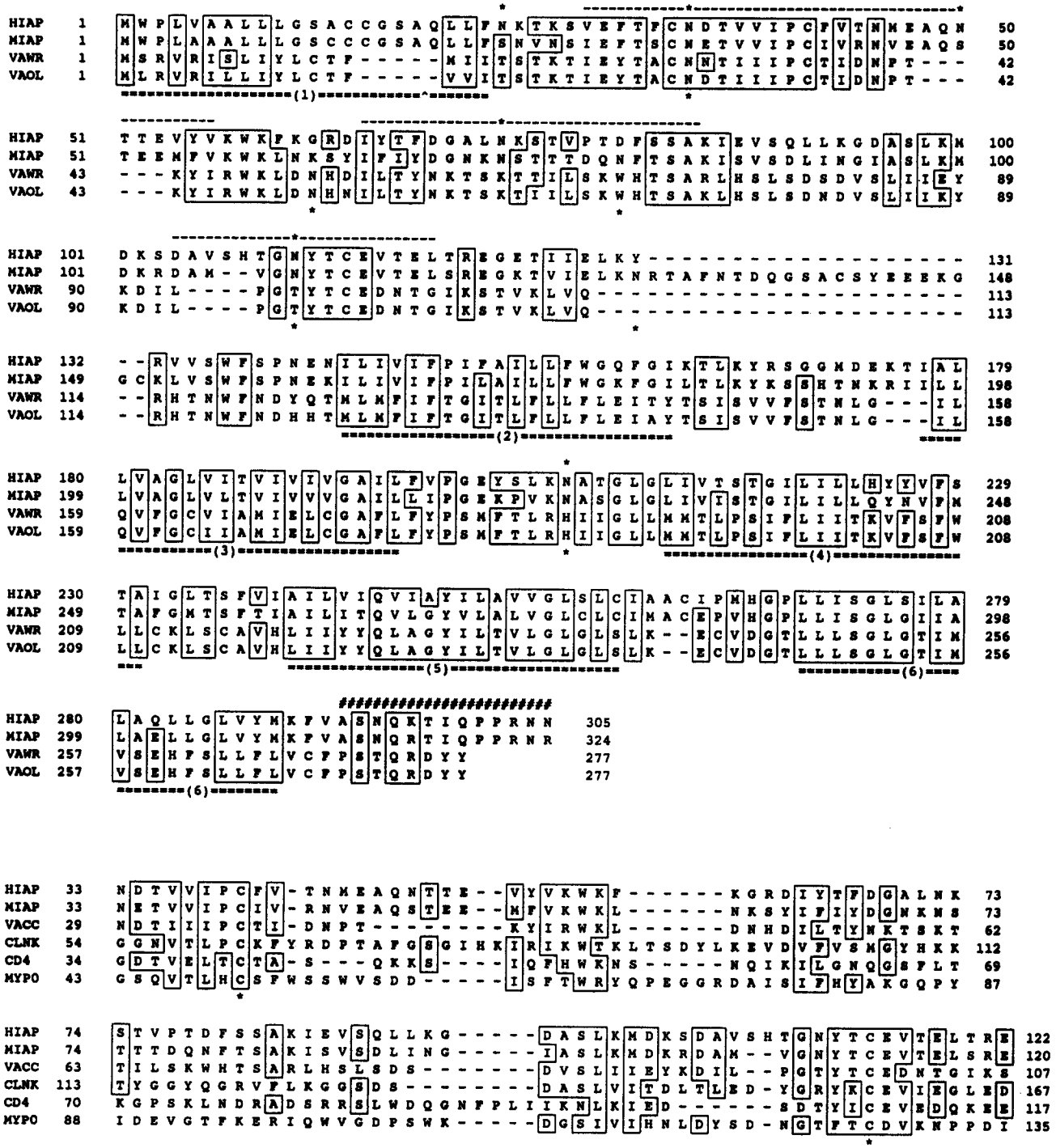

Figure 2. (*Top*) Amino acid sequence of human (*HIAP*) and murine (*MIAP*) IAP, as aligned with the vaccinia strain WR (37) and Variola (l) A38L proteins (*VAWR* and *VAOL*, respectively). Sequences are numbered starting with the initiator methionine. The amino acid sequences are given in the one-letter IUPAC code, with gaps introduced during the alignment indicated (−). Amino acids are boxed when the residues of three or four sequences are homologous at any given position. Apart from identities the following sets are considered to contain homologous amino acids: (*A, I, L, M, V*), (*K, R, H*), (*D, E*), (*S, T*), and (*Y, F*). Sequence obtained by Edman-degradation of tryptic IAP peptides are shown (----). The first of these was used to derive the oligonucleotides used in cloning. Potential N-linked glycosylation sites in the IAP sequences are shown by asterisks (*) above (human) or below (murine) the sequences. For all potential glycosylation sites contained within sequenced peptides, the yield of the asparagine (*N*) was very low, as would be expected if the residue is carbohydrate-linked. Hydrophobic potentially membrane-spanning segments are doubly underlined (====) and numbered, starting with the predicted signal peptide. The predicted signal peptide cleavage site is shown by a caret (Λ). The carboxy-terminal sequence used for the generation of peptide antisera is also shown (###). The human and murine cDNA sequences are available from Genbank (accession numbers Z25521 and Z25524). (*Bottom*) Alignment of the IgV-like regions from murine and human IAP with the most homologous members of the IgV family from Table I. The cysteine residues predicted to be disulfide linked in the IgV loop are marked by asterisks (*) below the sequences. Amino acids are boxed when the homology was between four or more of the sequences, according to the homology rules stated above.

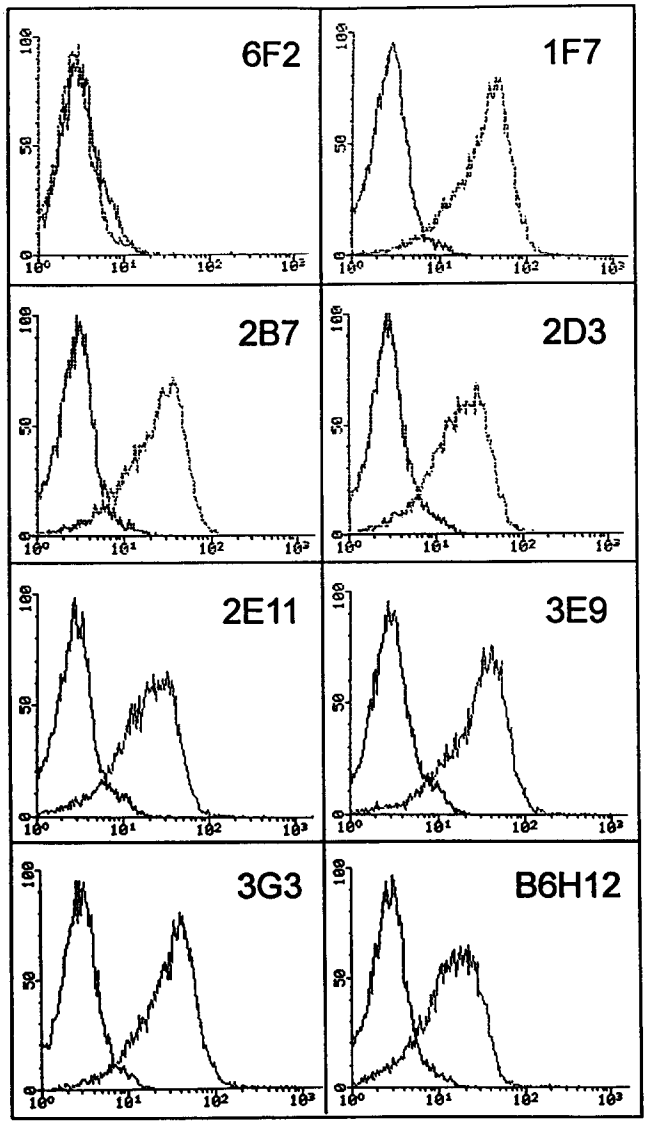

Figure 3. FACScan profiles for staining of CHO transfectants with various anti-IAP mAbs. The panels are designated by the respective antibody names. All antibodies are murine IgG1 anti-IAP mAbs, except 6F2, which is an isotype-matched negative control. The profiles shown are from CHO cells transfected with the human IAP-expressing construct pIAP45 (*dotted line, right hand curve*) and the non-expressing anti-sense control pIAP69 (*solid line, left hand curve*).

identical to IAP in terms of size and antibody reactivity (see below). The 3′ end of the coding region of the U937 clone had a 3′ [illegible]p deletion (singly underlined in Fig. 1) compared to the HL60 cDNAs, which leads to premature termination of the protein at Glu^{293}. This form also constitutes a very small minority of the clones obtained from the HL60 library. It presumably arose from alternative splicing of IAP mRNA, since both the sequence in the coding region 5′ to the deletion and the 3′ untranslated sequence of this cDNA are identical to those of the longer HL60 cDNAs.

Further evidence that the cDNAs encoded IAP was obtained by induction of anti-human IAP mAb reactivity with CHO cells after transfection with IAP cDNA (Fig. 3). This was confirmed by immunoprecipitation of an appropriate

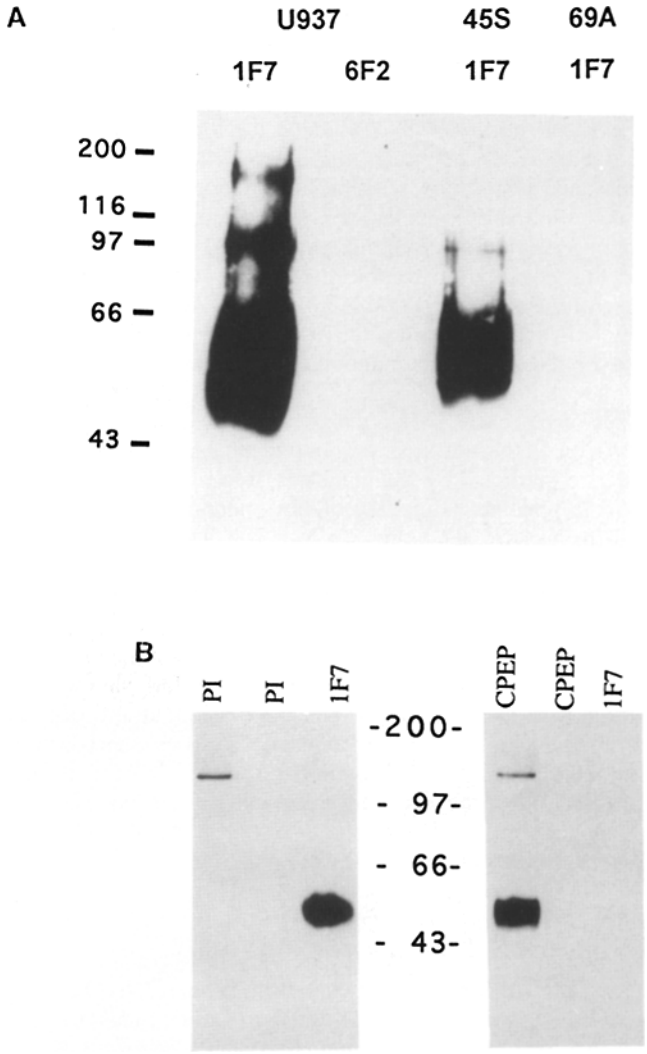

Figure 4. (*A*) Immunoprecipitation of human IAP from CHO cells transfected with the human IAP-expressing construct pIAP45 (*45S*) or the anti-sense control pIAP69 (*69A*). Human pro-myelocytic U937 cells (*U937*) were used as a positive control. Transfectants were grown to confluence in four 175 cm^2 flasks each, removed with PBS/2 mM EDTA, surface biotinylated, solubilized, and immunoprecipitated with anti-IAP mAb 1F7 or control mAb 6F2, as described in Materials and Methods. Under the conditions used (1% Triton X-100, 1% deoxycholate), coimmunoprecipitation with integrins is not seen. (*B*) Immunoprecipitation of IAP from human platelets with rabbit antiserum directed against the predicted carboxy terminus of human IAP. Platelets were surface biotinylated and solubilized. Immunoprecipitation was first carried out with a saturating amount of antibody directed against the peptide NQKTIQPPRNN, the predicted carboxy terminus of IAP, (*CPEP*) or preimmune serum (*PI*). A second round of immunoprecipitation was carried out with the same rabbit serum, and this immunoprecipitation revealed no antigen (second lane in each series). The supernatant of each series was used in immunoprecipitation again, this time with anti-IAP mAb 1F7. The anti-peptide antibody recognizes IAP and preclears all antigen recognized by mAb 1F7.

M_r band on SDS-PAGE from the transfected CHO with anti-IAP mAb (Fig. 4 *A*). Immunoprecipitations were done in 1% Triton X-100 and 1% deoxycholate, conditions under which integrin coimmunoprecipitation is not seen. To finally prove that the cDNA encoded IAP, we prepared an antibody

by immunizing rabbits with a synthetic peptide made from the predicted sequence of the IAP cDNA. This peptide, NQKTIQPPRNN, was the carboxy-terminal 11 amino acids of the sequence of the most common form of IAP cDNA in the HL60 library, which encoded the longer open reading frame. This anti-peptide antibody was used in sequential immunoprecipitation with 1F7, a previously characterized anti-IAP mAb (5). Under the conditions of cell lysis and immunoprecipitation, IAP migrates as a 50-kD protein on Superose 12 chromatography (data not shown), which is the size of the monomeric protein on SDS-PAGE. As shown in Fig. 4 *B*, antibody against the predicted sequence completely precleared all 1F7-immunoprecipitable IAP antigen from human platelets. Thus, the IAP cDNA encodes tryptic peptides of placental IAP, confers reactivity with all anti-IAP mAb on CHO cells, and antibody made against a peptide sequence predicted by the cDNA is able to recognize native IAP in platelets. Thus, the cDNA encodes IAP.

Murine IAP was cloned from a 70Z/3 pre-B cell cDNA library by homology to human IAP. Its predicted amino acid sequence is 71% identical and 87% similar to human IAP (Fig. 2). There is a 2-amino acid deletion and a 21-amino acid insertion in murine IAP relative to the human protein. The predicted carboxy terminus of murine IAP shows identity at 9 of 11 amino acids, and the polyclonal anti-peptide antibody made against the predicted human sequence immunoprecipitated a 48-kD protein from surface-labeled murine platelets, erythrocytes, and splenocytes (data not shown). Thus, the murine cDNA, like the human, encodes a widely expressed plasma membrane protein.

IAP Is Homologous to Poxvirus Proteins and Contains an Immunoglobulin Domain

When the IAP protein sequence was compared to Genbank sequences, human IAP was found to be identical to a recently cloned ovarian carcinoma antigen recognized by the mAb OVTL3 (7). The sole difference found was the absence in the OVTL-3 5′ untranslated sequence of the guanidine at position -85 of the human IAP cDNA sequence (Fig. 1). IAP is highly homologous to open reading frame A38L of the Vaccinia (alignment scores of 8.6 and 7.8 with human and murine IAP, respectively) and Variola major virus genomes (Fig. 2; *top*) (1, 12).

Kyte-Doolittle (39) hydrophobicity analysis (Fig. 5) indicates that IAP and A38L can be divided into a hydrophilic amino-terminal half and a hydrophobic carboxy-terminal domain. There is also an amino-terminal hydrophobic sequence which has the features of a signal peptide. Whether the amino terminus of IAP forms a transmembrane domain or is a signal sequence is currently unknown since the amino terminus of IAP purified from placenta, erythrocytes, and HL60, is blocked. The highly homologous A38L proteins have too few amino acids at their amino termini to form a membrane-spanning domain but these amino termini likely encode signal peptides. By analogy, the 20 amino acids at the amino terminus of IAP are likely to form a signal peptide. The blocked amino terminus of mature IAP may well begin with a pyrollidone carboxylic acid at Q^{19}.

The hydrophilic sequence after the putative signal peptide has three cysteines. The regions around the second and third of these show homology to the corresponding regions of several proteins in members the immunoglobulin superfamily.

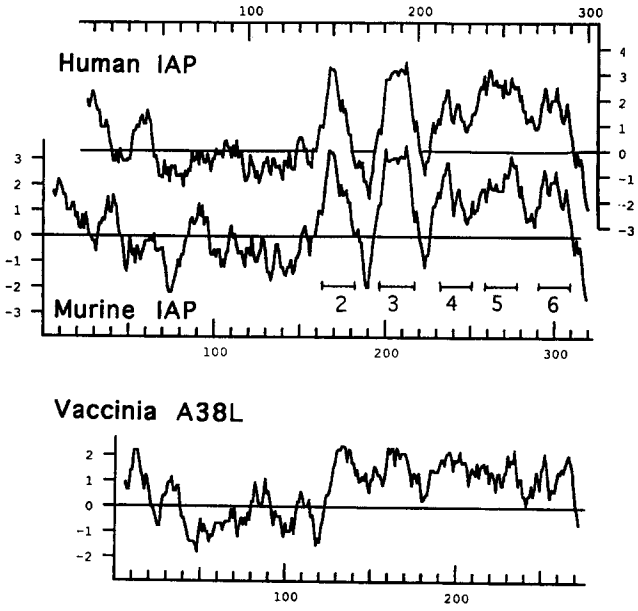

Figure 5. Assignment of membrane-spanning regions of IAP. Shown are hydrophobicity profiles (see Materials and Methods) for human and murine IAP, aligned by the carboxy-termini of the proteins. The horizontal axes are amino acid position in the respective protein and the vertical axes are arbitrary hydrophobicity units. The predicted membrane-spanning segments are indicated by horizontal bars numbered 2 through 6. The presumed signal peptide (membrane-spanning segment 1) is not shown. The lower half shows the vaccinia A38L hydrophobicity plot aligned with IAP by the membrane-spanning regions.

Further comparison shows that the amino terminus of IAP is most related to the IgV family, with significant homology to multiple family members (Table I; Fig. 2; *bottom*).

Anti-IAP mAbs Recognize the IgV-like Domain

Previous work has functionally characterized multiple anti-IAP mAb and demonstrated at least three distinct antigenic extracellular epitopes by crossinhibition and immunofluorescence studies (5). Therefore, we investigated which IAP domains are recognized by these various mAbs. Chimeric cDNAs were constructed which encoded hybrid proteins with the human immunoglobulin-like loop and murine transmembrane domain and the inverse construct encoding a murine immunoglobulin-like loop with human transmembrane domains. These chimeric constructs were transcribed and translated in vitro, and the translated products immunoprecipitated with anti-human IAP mAbs. As shown in Fig. 6, all seven anti-human mAb recognized proteins containing the human IgV-like domain, regardless of whether the rest of the molecule was murine or human sequence. The data were confirmed by FACS analysis of stable CHO transfectants expressing the same chimeric cDNA constructs (data not shown). These results demonstrate that this large hydrophilic domain is indeed extracellular.

IAP Membrane-spanning Segments

The carboxy-terminal hydrophobic regions of both IAP and the A38L proteins have five potential membrane-spanning segments (Fig. 5 and Fig. 2, *top*). Flanking segment 2 are basic residues to provide phospholipid anchoring (human

Table I. Alignment Scores for the Comparison of Human and Murine IAP to Vaccinia A38L and to Members of the IgV Immunoglobulin Superfamily

Sequence		HIAP	MIAP	VACC	CLNK	PIGR	HEAV	LAMB	CD4	CD8	OX-2	MYP0
Human IAP	HIAP											
Murine IAP	MIAP	15.0										
Vaccinia A38L	VACC	7.2	7.0									
Human cartilage link protein	CLNK	4.2	6.1	5.3								
Rabbit poly Ig receptor	PIGR	2.5	2.3	2.7	2.2							
Human Ig heavy chain	HEAV	2.8	3.4	2.5	2.7	2.4						
Mouse Ig lambda chain	LAMB	3.0	3.7	1.1	2.9	2.4	4.8					
Human CD4	CD4	4.3	3.5	5.1	3.6	5.3	2.2	4.1				
Rat CD8 beta	CD8	2.9	2.5	4.0	2.0	2.9	4.8	4.8	3.9			
Rat Ox-2	OX-2	2.5	2.7	1.8	1.9	2.2	0.8	2.3	1.4	2.4		
Rat myelin P0	MYP0	4.4	3.2	2.7	5.7	3.6	2.8	0.3	4.6	2.3	2.4	
Rat Thy-1	THY1	3.2	2.6	2.8	2.5	2.4	1.1	3.4	3.8	3.0	4.9	2.4

Sequences were aligned using the Needleman and Wunsch algorithm (10) using the PAM250 protein alignment matrix, with a bias of 10 and a gap penalty of 10. The score obtained for each pair was compared to that obtained aligning 150 random permutations of the sequences. The real score is expressed as standard deviations above the mean of the random scores. Sequences were obtained from the Swiss Protein Database. The comparison was performed using sequences from 7 amino acids before the first cysteine through position 8 after the second cysteine forming the known or predicted disulfide bond. The sequences are Human IAP (residues 33–122), murine IAP (33–120), Vaccinia A38L (29–107) accession number P24768 (12), human cartilage link protein (54–167) X17405 (19). The other sequences were used in Williams and Barclay (36) to define the IgV family and are referenced there. The accession numbers and residues included in the comparison are Rabbit polymeric Ig receptor precursor second IgV-like domain P01832 and 148–233, human Ig heavy chain variable region P01825 and 15–103, mouse Ig lambda chain variable region P01724 and 34–117, human CD4 IgV-like domain P01730 and 34–117, rat CD8 beta chain IgV-like domain P05541 and 34–123, rat ox-2 glycoprotein P04218 and 44–129, rat myelin P0 protein P06907 and 43–135, rat Thy-1 antigen P01830 and 21–122.

K^{163}/K^{165}, mouse K^{161}/K^{184}). Similarly, there are K^{175} and R^{194} at the amino-terminal border of segment 3, and K^{290} and K^{310} at the carboxy-terminal border of segment 6. Segment 5 is similarly delimited in the A38L proteins, with very high homology to IAP in this region, as is the carboxy-terminal end of segment 4. The presence of strongly helix breaking H^{224} in human segment 4 (Fig. 2; *top*) and the relative hydrophobicity of the region between segments 4 and 5, make the assignment of segment 4 more tentative. This segment alone or together with segment 5 could be a membrane-associated rather than membrane-spanning region.

Immunolocalization of the IAP Carboxy Terminus

Since the total number of membrane-spanning segments after the IgV domain would affect the localization of the carboxy-terminal hydrophilic peptide, we decided to determine whether the carboxy terminus is located on the inside

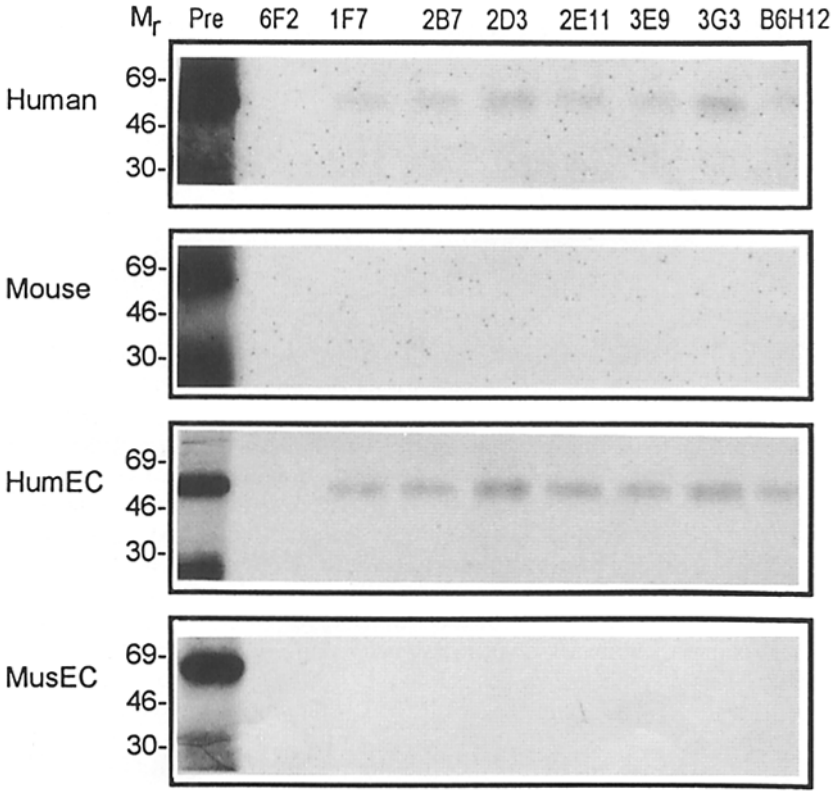

Figure 6. In vitro translation of human-mouse chimeric IAPs and immunoprecipitation with different IAP mAbs. The IAPs were human (*Human*), murine (*Mouse*), murine with human hydrophilic domain (*HumEC*), or human with murine hydrophilic domain (*MusEC*). The recombination point between the hydrophilic domain and the carboxy-terminal remainder of the molecule was at W^{135} (human numbering, see Fig. 1). The [^{35}S]methionine labeled in vitro synthesized IAPs were immunoprecipitated with the various IAP antibodies (*B6H12*, *1F7*, *2B7*, *2D3*, *2E11*, *3E9*, or *3G3*) or negative isotype-matched control antibody (*6F2*).

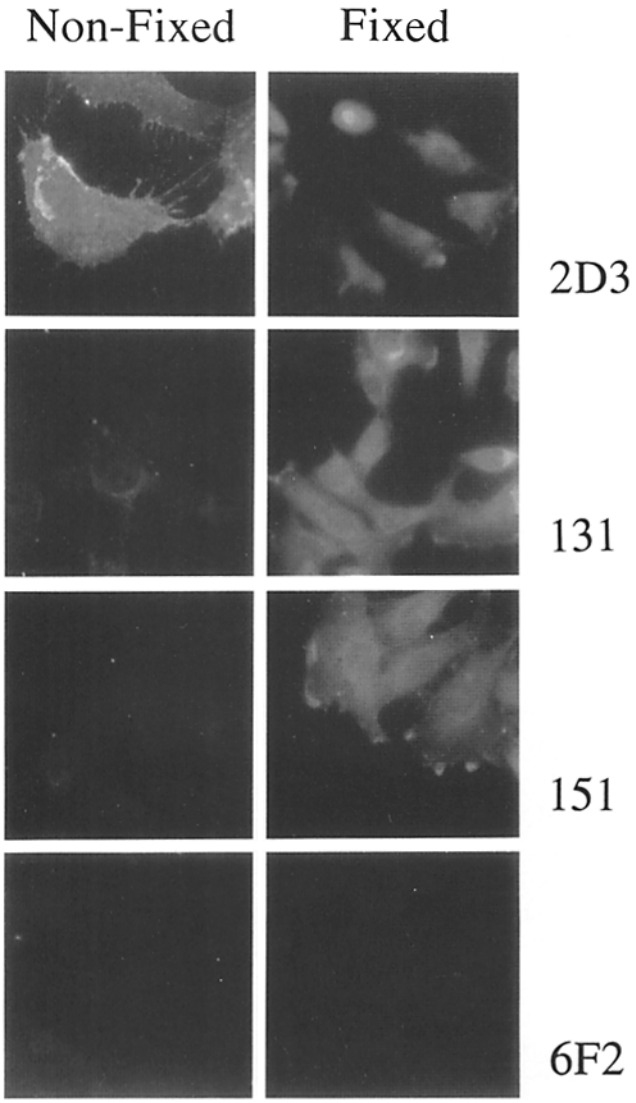

Figure 7. Immunolocalization of the human IAP carboxy terminus in human T24 cells. Cells adherent to glass slides were stained with murine anti-human IAP mAb 2D3 (*2D3*) reacting with the extracellular aspect of IAP, with miap131 (*131*) or miap151 (*151*) reacting with the carboxy terminus, or with the irrelevant control mAb 6F2 (*6F2*). The left hand column shows fluorescence micrographs of cells stained before methanol treatment (*non-fixed*). The right hand micrographs are of cells stained after permeabilization/fixation with methanol (*fixed*). The anti-carboxy terminus mAbs stain only permeabilized cells suggesting that the epitope is located intracellularly. Isolated membranes from T24 cells also showed specific staining with these mAbs (data not shown).

or outside of the cytoplasmic membrane. Human T24 uroepithelial carcinoma cells were stained with or without prior permeabilization with methanol with mouse mAbs miap131 and miap151 against the human IAP carboxy terminus (see Materials and Methods). As controls, 2D3 binding to extracellular parts of IAP and negative antibody 6F2 were used. As shown in Fig. 7, both miap131 and miap151 stain T24 cells only after methanol permeabilization, suggesting that the carboxy terminus is located in the cytoplasm. This in turn implies that the carboxy-terminal hydrophobic domain of IAP must encode an odd number of membrane-spanning segments.

Structural Model for IAP

From this information a structural model of IAP was made (Fig. 8). This model predicts a protein with an amino-terminal IgV-like extracellular domain and a carboxy-terminal multiply membrane-spanning domain. The IgV-like domain contains all but one predicted N-glycosylation sites. At least four of these sites are used, since amino acid sequencing of tryptic peptides from IAP purified from placenta gave very low yields at the predicted Asn. The IgV homology suggests the disulfide linkage shown in Fig. 8, although its presence has not been shown experimentally. Since the IgV-like domain is extracellular and the carboxy terminus intracellular, the carboxy-terminal hydrophobic domain has an odd number of membrane-spanning segments. The hydropathy plot of this region is consistent with 5 transmembrane domains as shown. However, the assignment of segment 4 (third transmembrane segment in Fig. 8) is more tentative due to the lack of a basic phospholipid anchoring amino acid and the presence of a histidine near the center of the segment. If segment 4 is not membrane spanning, this would have to be true also of segment 3 or 5. The strongly hydrophobic character of these regions of IAP suggest that they would be membrane-associated if not membrane-spanning.

Anti-IAP Inhibits $\alpha_v\beta_3$-dependent Ligand Binding

IAP is a widely expressed protein, present on many cell types and was initially copurified with $\alpha_v\beta_3$ from placenta. Anti-IAP antibodies inhibit binding of multivalent RGD- and KGAGDV-peptides to polymorphonuclear cells (PMN) (16, 17), but careful study of the functional effect of these antibodies has been limited to this genetically nonmanipulatable system. To determine whether anti-IAP mAb might affect $\alpha_v\beta_3$ function, we examined the binding of Vn- and Fn-coated beads to HEL cells, which are known to express $\alpha_v\beta_3$ and $\alpha_5\beta_1$. Anti-IAP mAb B6H12, which inhibits ligand bead binding to PMN (16), inhibited the binding of Vn-beads but not Fn-beads to these cells (Fig. 9). Anti-IAP mAb 2D3, which does not inhibit ligand-bead binding to PMN, also did not inhibit Vn-bead binding to HEL cells. Binding of Vn-beads was inhibited both by polyclonal anti-$\alpha_v\beta_3$ and by the anti-β_3 mAb 7G2. These data demonstrate that anti-IAP mAb can inhibit Vn binding to $\alpha_v\beta_3$, but does not affect Fn binding to $\alpha_5\beta_1$ on the same cells.

Anti-Human IAP mAb Inhibit Vitronectin Receptor Function in Transfected CHO Cells

We used the ability of anti-IAP to inhibit Vn binding to α_v integrin receptors to examine the function of transfected human IAP in CHO cells, using mAbs that recognized only the transfected human molecule. In these cells transfected with IAP cDNA, half or less of the total expressed IAP was human, as judged by alteration in binding of polyclonal anti-IAP (Fig. 10 *A*). Polyclonal anti-human IAP recognized hamster IAP (Fig. 10 *A*) and inhibited binding of Vn-beads to untransfected CHO cells and CHO cells transfected with the control reverse cDNA (Fig. 10 *B*). In contrast, anti-human IAP mAb neither recognized these CHO cells nor affected Vn-beads binding. In CHO cells expressing human IAP, as in HEL cells, B6H12 inhibited Vn-beads binding as completely as polyclonal anti-IAP (see Discussion). Again, as for HEL cells, 2D3 did not affect Vn-bead binding (Fig.

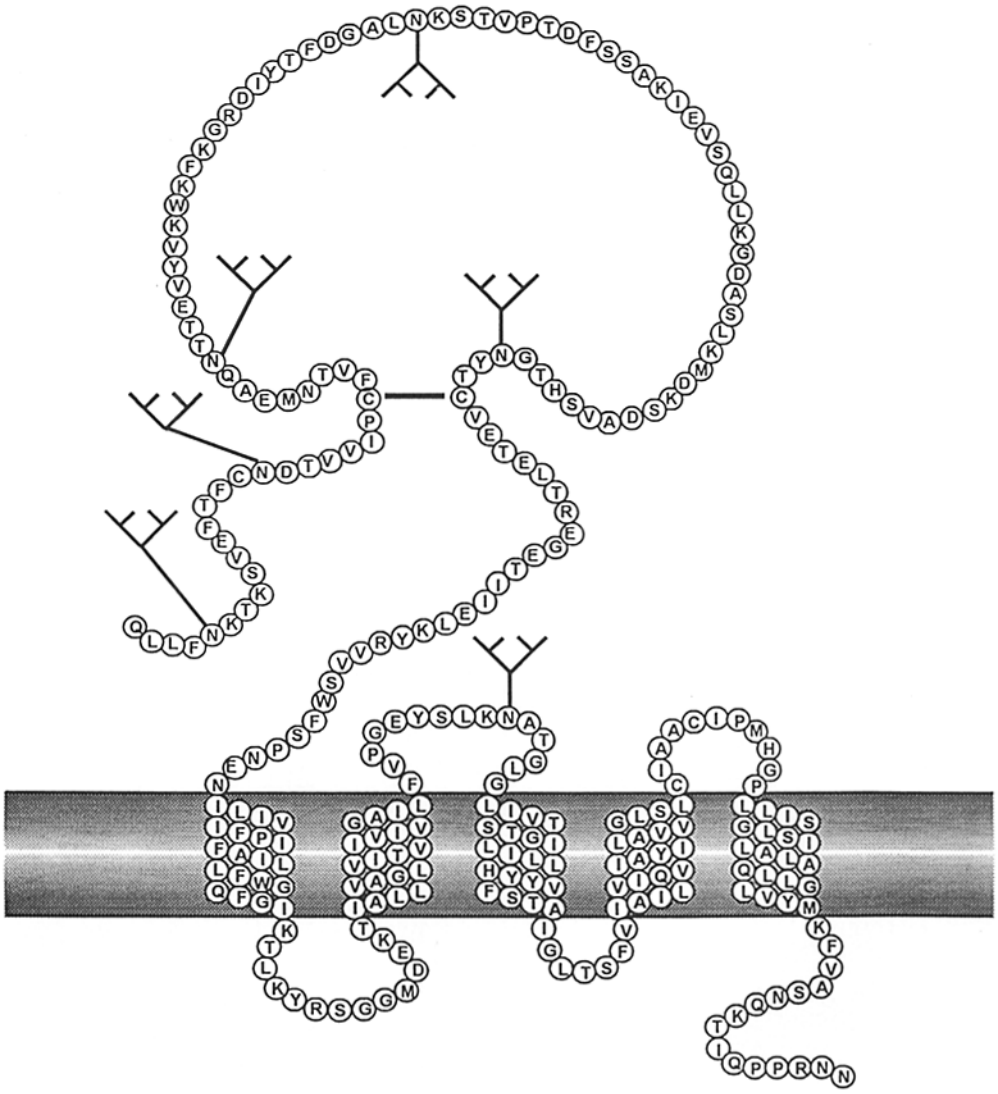

Figure 8. Structural model for human IAP. The model is based on predictions from the primary sequence, as derived from the cDNA sequence, as well as homology to known members of the immunoglobulin superfamily. The potential N-linked glycosylation sites are shown, and are presumed to be extracellular. Low yields of the corresponding asparagines by amino acid sequencing suggests that at least the second through fourth potential glycosylation sites carry carbohydrate. The hydrophilic region has considerable similarity to immunoglobulin variable regions. The disulfide linkage suggested by this homology is indicated, but its presence or absence has not been experimentally investigated. The carboxy terminus is located on the inside of the cell membrane. The assignment of membrane-spanning segments is tentative and it is possible that the third segment is membrane-associated rather than membrane-spanning. In this case, this would have to be true for at least one other hydrophobic segment, since an odd number of transmembrane regions would be required to connect the extracellular IgV domain to the intracellular carboxy terminus.

10 *B*). Fn-beads binding to CHO cells was not inhibited by monoclonal or polyclonal anti-IAP antibodies in the transfectants or the control cells (data not shown). These data suggest that human IAP can associate with hamster α_v receptor(s).

Discussion

We have previously described a 50-kD protein which copurified with $\alpha_v\beta_3$ from placenta and which coimmunoprecipitated with β_3 integrins from platelets. Because of this, we called this protein the Integrin Associated Protein, IAP. Now, we have cloned IAP cDNA. The proof that the cloned molecule is IAP is that (*a*) several tryptic peptides derived from native placental IAP are found in the predicted amino acid sequence of the clone; (*b*) the product of in vitro transcription/translation of the cloned cDNA is recognized by all anti-IAP mAb; (*c*) transfection of the human cDNA into CHO cells confers reactivity with mAb specific for human IAP on the transfectants; and (*d*) immunoprecipitation with a cDNA sequence derived carboxy-terminal peptide antibody preclears all IAP reactivity from a platelet lysate. The predicted amino acid sequence of the cDNA is highly hydrophobic and predicts a molecule with a single extracellular IgV-like domain and multiple membrane-spanning segments. Because immunoglobulin domains are often involved in intermolecular interactions, this structure suggests the hypothesis that the extracellular domain is important in the interaction of IAP with its associated integrins. The relative lack of conservation of the extracellular domain between mouse and human IAP (61% compared to 77% in the multiple transmembrane domains) is still consistent with this hypothesis, since the amino acid sequence of ICAM-1, another immunoglobulin superfamily molecule which interacts with integrins, is even less conserved between these species (20).

The sequence of IAP is identical to the sequence of a recently cloned ovarian carcinoma antigen (7). This antigen was cloned because it was recognized by an "ovarian carcinoma-specific" antibody, OVTL3 (3, 29). We cannot explain why IAP, which is ubiquitously expressed, was thought to be a carcinoma-specific antigen. Campbell et al. report that mRNA for this protein is present in all normal tissues tested (7). In our hands (data not shown), as well as for Campbell et al. (7), OVTL3 recognizes IAP on several

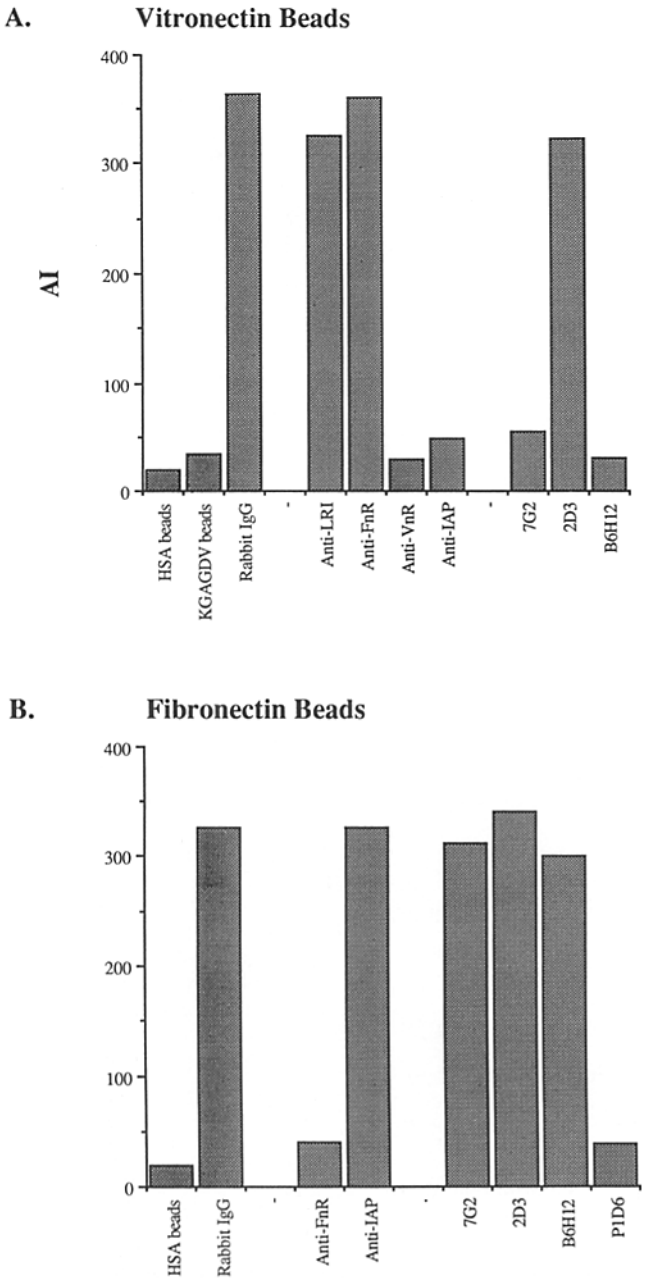

Figure 9. (*A*) Binding of Vn-beads to HEL cells. The ability of HEL cells to recognize and attach ligand-coated beads was assessed as described in Materials and Methods. Attachment was quantitated as attachment index (*AI*), the number of beads bound/100 cells. Control represents binding in the presence of non-immune rabbit IgG, which is not different from buffer alone. Anti-IAP (5), anti-LRI (8), and anti-VnR are IgG fractions of rabbit antisera. 2D3 and B6H12 are IgG1 anti-IAP mAb, and 7G2 is IgG1 anti-β_3 mAb. The experiment shown is representative of at least six repetitions for each antibody. Controls included KGAGDV-beads (a ligand specific for LRI [17]) and HSA beads. These experiments demonstrate that both $\alpha_v\beta_3$ and IAP were required for Vn-beads binding by HEL cells. (*B*) Binding of Fn-beads to HEL cells. These experiments were performed as in *A*, except that the ligand coating on the bead was Fn and the incubation buffer differed in divalent cation content (see Materials and Methods). The binding of Fn-beads to HEL was dependent on $\alpha_5\beta_1$ but was independent of IAP.

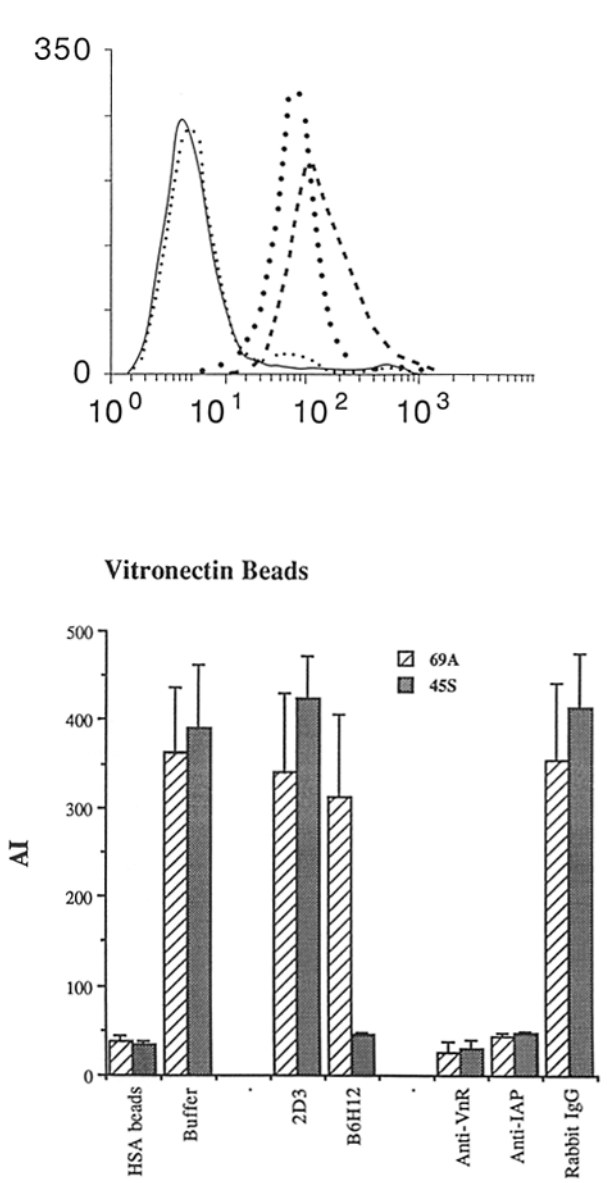

Figure 10. (*A*) Fluorescence flow cytometry of CHO cells transfected with human IAP cDNA. CHO cells were transfected with constructs of either full length human IAP cDNA (*pIAP45*) (*solid line*, *dashed line* [---]) or of anti sense cDNA (*pIAP69*) as a control (*small* and *large dotted lines* [•, •]), as in Figs. 3 and 4 *A*. The CHO cells were analyzed by fluorescence flow cytometry using polyclonal anti-IAP (5) (•, ---) or preimmune serum (•, *solid line*). Both the human IAP transfectant and the control are recognized by the polyclonal anti-IAP. The human IAP transfectant has a mean fluorescence with anti-IAP about twice that of the control. (*B*) Binding of Vn-beads to CHO transfectants. CHO cells, transfected with either human IAP cDNA (*45S*) or anti-sense (*69A*), as in *A*, were tested for their binding of Vn-beads in the presence of the same antibodies tested in Fig. 9. Data are the mean ± SD for three independent experiments done in duplicate. Attachment was quantitated as AI (see Materials and Methods). B6H12, which recognizes only human IAP, completely inhibits Vn-beads binding to 45S cells, even though it does not recognize hamster IAP.

different cells, including CHO cells transfected with human IAP cDNA. Perhaps the specificity has a quantitative rather than qualitative basis. IAP also is homologous to the expected product of the poxvirus A38L reading frame (1, 12,

37). Interestingly, the A38L product also has an amino-terminal unpaired cysteine, which could form disulfide bonds with other molecules. However, we have not seen covalent interaction of IAP with itself or with any other proteins. The high degree of conservation of the IAP homologue between Vaccinia and Variola suggests that this protein has an important role in the viral life cycle. Many viral proteins have been shown to influence pathogenesis by mimicking or inhibiting host molecules (13). The function of this viral protein remains unknown.

The multiple membrane-spanning domains in the carboxy terminus of IAP suggest several testable possible roles for IAP in signal transduction. One possibility is that this region of IAP has a transporter or channel function. In this regard, adhesion of endothelial cells to vitronectin or fibronectin causes an increase in $[Ca^{+2}]_i$ (34), which can be blocked by B6H12, but not 2D3, suggesting that IAP is involved in the signaling for Ca^{+2} entry into the cells (34*a*). However, as yet, we have no direct experimental data to support the hypothesis that IAP can itself act as a membrane channel.

IAP was defined originally as the target of a monoclonal antibody, B6H12, which inhibited the function of a leukocyte β_3-like integrin, the LRI. Functional inhibition by B6H12 involved its ability to block ligand binding to LRI (16, 17). In the current study, we have shown that anti-IAP also can block ligand binding to the much better characterized Vn receptor, $\alpha_v\beta_3$, on HEL cells and to α_v receptors on CHO cells. Moreover, binding of Vn-coated particles to CHO cells transfected with human IAP was completely inhibited by B6H12, which recognizes human but not hamster IAP. This dominant effect of the anti-human IAP mAb is very surprising in view of the presence of non-inhibited hamster IAP on these cells. This would be expected if B6H12-bound IAP binds to the integrin in an inhibitory fashion. B6H12 may stabilize a conformation of human IAP which favors physical and functional association with CHO $\alpha_v\beta_3$. We have previously shown that IAP is capable of existing in two conformational states with different affinities for B6H12 (30). Another possibility is that the antibody to IAP might generate a signal inhibitory to $\alpha_v\beta_3$ and LRI ligand binding, independent of its ability to associate with these integrins. This would have to be a very specific negative signal, since binding of Fn-coated beads to another integrin on the same cells is unaffected by B6H12. In addition, kinetic studies of Vn-bead binding to HEL cells indicate that the initial rate of Vn binding is unaffected by B6H12 (Gresham, H. D., unpublished observation). If the antibody were simply activating a negative signal, even one specific for $\alpha_v\beta_3$, this would not be expected. Furthermore, data obtained with PMN show that B6H12 but not 2D3 can stimulate the respiratory burst when adherent to a tissue culture plate and that this respiratory burst is inhibited by anti-LRI mAb and LRI ligands in solution (41). These data favor the possibility that B6H12 can stabilize a signal transduction complex which contains both LRI and IAP, suggesting a model in which IAP association with integrins is dynamic, possibly affected by integrin ligands or other environmental influences on cell phenotype and by some anti-IAP mAbs. Notably, cytokine receptor complexes often contain a transmembrane protein which is not directly involved in ligand binding but which is critical for high affinity ligand binding and signal transduction (11, 23, 26, 28). Gp130 functions in this way as a component of the IL6 and LIF receptors, as does the β chain of the IL3, IL5, and GM-CSF receptors (14, 18 23, 28, 38). In at least one case, that of gp130, ligand is required to stabilize the association of this additional chain with the ligand binding subunit of the IL6 receptor (18, 38). At this time, the association of gp130 with the IL6 receptor appears to be a reasonable model for the association of IAP with LRI and $\alpha_v\beta_3$. The existence of at least one other immunoglobulin superfamily member which modulates integrin binding of ligands (21) suggests that IAP-like molecules may be a general mechanism involved in integrin dependent signal transduction.

The authors thank Matt Williams for skillful technical assistance; the Washington University Protein Chemistry facility for peptide sequencing, peptide synthesis, and oligonucleotide synthesis; Dave McCourt for peptide sequencing; Jeff Millbrandt, Matt Thomas, and James Matthews for help designing and executing the initial PCR cloning strategy; Matt Thomas and Neil Barclay for helpful comments; Brian Volpp and Doug Lublin for providing cDNA libraries; and multiple members of the Brown lab for helpful suggestions and critical reading of the manuscript. We are also very grateful to the reviewers for their comments on membrane assignments.

This work was supported by National Institutes of Health grant GM38330, the Medical Research Service of the Department of Veterans Affairs, and the Washington University-Monsanto Corporation Biomedical Agreement. FPL is supported by a postdoctoral fellowship of the Howard Hughes Medical Institute.

Received for publication 16 June 1993 and in revised form 22 July 1993.

References

1. Aguado, B., I. P. Selmes, and G. L. Smith. 1993. Nucleotide sequence of 21.8 kbp of variola major virus strain Harvey and comparison with vaccinia virus. *J. Gen. Virol.* 73:3887–2902.
2. Aota, S., T. Nagai, K. Olden, S. K. Akiyama, and K. M. Yamada. 1991. Fibronectin and integrins in cell adhesion and migration. *Biochem. Soc. Trans.* 19:830–835.
3. Boerman, O. C., C. van Niekerk, K. Makkink, T. G. J. M. Hanselaar, P. Kenemans, and L. G. Poels. 1991. Comparative immunohistochemical study of four monoclonal antibodies directed against ovarian carcinoma-associated antigens. *Int. J. Gynecol. Path.* 10:15–25.
4. Brown, E. J., and F. P. Lindberg. 1993. Matrix receptors of myeloid cells. *In* Blood Cell Biochemistry, Macrophages and Related Cells. Vol. 5. M. A. Horton, editor. Plenum Press, New York. 279–306.
5. Brown, E. J., L. Hooper, T. Ho, and H. D. Gresham. 1990. Integrin-associated protein: a 50-kD plasma membrane antigen physically and functionally associated with integrins. *J. Cell Biol.* 111:2785–2794.
6. Burridge, K., G. Nuckolls, C. Otey, F. Pavalko, K. Simon, and C. Turner. 1990. Actin-membrane interaction in focal adhesions. *Cell Differ. Dev.* 32:337–342.
7. Campbell, I. G., P. S. Freemont, W. Foulkes, and J. Trowsdale. 1992. An ovarian tumor marker with homology to vaccinia virus contains an IgV-like region and multiple transmembrane domains. *Cancer Res.* 52: 5416–5420.
8. Carreno, M. P., H. D. Gresham, and E. J. Brown. Isolation of the leukocyte response integrin (LRI): a novel RGD-binding protein involved in regulation of phagocyte function. *Clin. Immunol. Immunopathol.* In Press.
9. Cleveland, D. W., S. G. Fischer, M. W. Kirschner, and U. K. Laemmli. 1977. Peptide mapping by limited proteolysis in sodium dodecylsulfate and analysis by gel electrophoresis. *J. Biol. Chem.* 252:1102–1106.
10. Duyster, J., H. Schwende, E. Fitzke, H. Hidaka, and P. Dieter. 1993. Different roles of protein kinase C-β and -δ in arachidonic acid cascade, superoxide formation and phosphoinositide hydrolysis. *Biochem. J.* 292:203–207.
11. Gearing, D. P., et al. 1992. The IL-6 signal transducer, gp130: an oncostatin M receptor and affinity converter for the LIF receptor. *Science (Wash. DC).* 255:1434–1437.
12. Goebel, S. J., G. P. Johnson, M. E. Perkus, S. W. Davis, J. P. Winslow, and E. Paoletti. 1990. The complete DNA sequence of vaccinia virus. *Virology.* 179:247–266.
13. Gooding, L. R. 1992. Virus proteins that counteract host immune defenses. *Cell.* 71:5–7.
14. Gorman, D. M., N. Itoh, N. A. Jenkins, D. J. Gilbert, N. G. Copeland, and A. Miyajima. 1992. Chromosomal localization and organization of the murine genes encoding the beta subunits (AIC2A and AIC2B) of the interleukin 3, granulocyte/macrophage colony-stimulating factor, and in-

terleukin 5 receptors. *J. Biol. Chem.* 267:15842–15848.
15. Graham, F. L., and A. J. Van Der Eb. 1973. A new technique for the assay of infectivity of human adenovirus 5 DNA. *Virology.* 52:456–461.
16. Gresham, H. D., J. L. Goodwin, D. C. Anderson, and E. J. Brown. 1989. A novel member of the integrin receptor family mediates Arg-Gly-Asp-stimulated neutrophil phagocytosis. *J. Cell Biol.* 108:1935–1943.
17. Gresham, H. D., S. P. Adams, and E. J. Brown. 1992. Ligand binding specificity of the leukocyte response integrin expressed by human neutrophils. *J. Biol. Chem.* 267:13895–13902.
18. Hibi, M., M. Murakami, M. Saito, T. Hirano, T. Taga, and T. Kishimoto. 1990. Molecular cloning and expression of an IL-6 signal transducer, gp130. *Cell.* 63:1149–1157.
19. Hill, H. R., N. H. Augustine, P. A. Williams, E. J. Brown, and J. F. Bohnsack. 1993. Mechanism of fibronectin enhancement of group B streptococcal phagocytosis by human neutrophils and culture-derived macrophages. *Infect. Immun.* 61:2334–2339.
20. Horley, K. J., C. Carpenito, B. Baker, and F. Takei. 1989. Molecular cloning of murine intercellular adhesion molecule (ICAM-1). *EMBO (Eur. Mol. Biol. Organ.) J.* 8:2889–2896.
21. Huang, R.-P., M. Ozawa, K. Kadomatsu, and T. Muramatsu. 1993. Embigin, a member of the immunoglobulin superfamily expressed in embryonic cells, enhances cell-substratum adhesion. *Dev. Biol.* 155: 307–314.
22. Hynes, R. O. 1992. Integrins: versatility, modulation, and signaling in cell adhesion. *Cell.* 69:11–25.
23. Kitamura, T., N. Sato, K. Arai, and A. Miyajima. 1991. Expression cloning of the human IL-3 receptor cDNA reveals a shared beta subunit for the human IL-3 and GM-CSF receptors. *Cell.* 66:1165–1174.
24. Kozak, M. 1984. Compilation and analysis of sequences upstream from the translational start site in eukaryotic mRNAs. *Nucleic Acids Res.* 12:857–870.
25. Langdale, L. A., L. C. Flaherty, H. D. Liggitt, J. M. Harlan, C. L. Rice, and R. K. Winn. 1993. Neutrophils contribute to hepatic ischemia-reperfusion injury by a CD18-independent mechanism. *J. Leukocyte Biol.* 53:511–517.
26. Liu, J., B. Modrell, A. Aruffo, J. S. Marken, T. Taga, K. Yasukawa, M. Murakami, T. Kishimoto, and M. Shoyab. 1992. Interleukin-6 signal transducer gp130 mediates oncostatin M signaling. *J. Biol. Chem.* 267: 16763–16766.
27. Lublin, D. M., M. K. Liszewski, T. W. Post, M. A. Arce, M. M. LeBeau, M. B. Rebentisch, L. S. Lemons, T. Seya, and J. P. Atkinson. 1988. Molecular cloning and chromosomal localization of human membrane cofactor protein (MCP). Evidence for inclusion in the multigene family of complement-regulatory proteins. *J. Exp. Med.* 168:181–194.
28. Nicola, N. A., and D. Cary. 1992. Affinity conversion of receptors for colony stimulating factors: properties of solubilized receptors. *Growth Factors.* 6:119–129.
29. Poels, G., D. Peters, Y. van Megen, et al. 1986. Monoclonal antibody against human ovarian tumor-associated antigens. *JNCI (J. Nat. Cancer Inst.)* 76:781–787.
30. Rosales, C., H. D. Gresham, and E. J. Brown. 1992. Expression of the 50 kD integrin associated protein on myeloid cells and erythrocytes. *J. Immunol.* 149:2759–2764.
31. Ruoslahti, E. 1991. Integrins. *J. Clin. Invest.* 87:1–5.
32. Sambrook, J., E. F. Fritsch, and T. Maniatis. 1989. Molecular Cloning: A Laboratory Manual. 2nd Ed. Cold Spring Harbor Laboratory Press, Cold Spring Harbor, NY.
33. Sanger, F., S. Nicklen, and A. R. Coulson. 1977. DNA sequencing with chain-terminating inhibitors. *Proc. Natl. Acad. Sci. USA.* 74:5463–5467.
34. Schwartz, M. A. 1993. Spreading of human endothelial cells on fibronectin or vitronectin triggers elevation of intracellular free calcium. *J. Cell Biol.* 120:1003–1010.
34*a*. Schwartz, M. A., E. J. Brown, and B. Fayeli. A 50 kDa integrin-associated protein is required for integrin-regulated calcium entry in endothelial cells. *J. Biol. Chem.* In press.
35. Senior, R. M., H. D. Gresham, G. L. Griffin, E. J. Brown, and A. E. Chung. 1992. Entactin stimulates neutrophil adhesion and chemotaxis through interactions between its Arg-Gly-Asp (RGD) domain and the leukocyte response integrin (LRI). *J. Clin. Invest.* 90:2251–2257.
36. Shaw, L. M., M. M. Lotz, and A. M. Mercurio. 1993. Inside-out integrin signaling in macrophages. Analysis of the role of the $\alpha 6A\beta 1$ and $\alpha 6B\beta 1$ integrin variants in laminin adhesion by cDNA expression in an $\alpha 6$ integrin-deficient macrophage cell line. *J. Biol. Chem.* 268:11401–11408.
37. Smith, G. L., Y. S. Chan, and S. T. Howard. 1991. Nucleotide sequence of 42 kbp of vaccinia virus strain WR from near the right inverted terminal repeat. *J. Gen. Virol.* 72:1349–1376.
38. Taga, T., M. Hibi, Y. Hirata, et al. 1989. Interleukin-6 triggers the association of its receptor with a possible signal transducer, gp130. *Cell.* 58:573–581.
39. Vidal, S. M., D. Malo, K. Vogan, E. Skamene, and P. Gros. 1993. Natural resistance to infection with intracellular parasites: isolation of a candidate for *Bcg*. *Cell.* 73:469–485.
40. Volpp, B. D., W. M Nauseef, J. E. Donelson, D. R. Moser, and R. A. Clark. 1989. Cloning of the cDNA and functional expression of the 47-kilodalton cytosolic component of human neutrophil respiratory burst oxidase. *Proc. Natl. Acad. Sci. USA.* 86:7195–7199.
41. Zhou, M.-J., and E. J. Brown. 1993. Leukocyte response integrin and integrin associated protein act as a signal transduction unit in generation of a phagocyte respiratory burst. *J. Exp. Med.* 178:1165–1174.